SF_6 mixed in N_2 gas sensing responses from CMOS compatible AlN and ScAlN pyroelectric detectors

Doris K. T. Ng*[a], Weiguo Chen[a], Linfang Xu[a], Harmony J. E. Lau[a], Landobasa Y. M. Tobing[a], Chong Pei Ho [a], Wing Wai Chung [a], Norhanani Jaafar [a], Hanfeng Fu [a], Qingxin Zhang [a]
[a]Institute of Microelectronics (IME), Agency for Science, Technology and Research (A*STAR), 2 Fusionopolis Way, Innovis #08-02, Singapore 138634, Republic of Singapore

ABSTRACT

SF_6 gas sensor is developed to measure SF_6 gas at different concentrations mixed with N_2 based on mid-IR absorption of SF_6 at a wavelength of ~10.6 µm. An optical bandpass filter of ~10.6 µm is put in front of a thermal emitter source to allow light of this wavelength to pass through. A CMOS compatible pyroelectric detector is put on the other end of the gas channel to measure the voltage change due to presence of SF_6 gas. Here, we use AlN-based and 12% ScAlN-based pyroelectric detectors respectively. The results show for 100% SF_6 gas sensing, 12% ScAlN-based pyroelectric detector gives ~73% higher response compared to when using AlN-based pyroelectric detector. The voltage drop between reference N_2 gas and different SF_6 gas concentrations is also higher (up to 2x) when using 12% ScAlN-based pyroelectric detector. Based on the measured SF_6 gas responses, we try to estimate the lower limit of detection of our gas sensors when using AlN- and ScAlN- based pyroelectric detectors respectively. Response times taken for both detectors to detect SF_6 concentrations are measured to be ~6.26 s for AlN-based pyroelectric detector and ~1.99 s for 12% ScAlN-based pyroelectric detector. Finally, both pyroelectric detectors' electrical responses across different frequencies are measured and their 3-dB frequency cutoffs are extracted to be ~13.5 Hz and ~12.6 Hz for AlN- and 12% ScAlN- based pyroelectric detector respectively. The results provide more understanding on characteristics of pyroelectric detectors in SF_6 greenhouse gas sensing based on mid-IR absorption.

Keywords: greenhouse gases, SF_6 gas sensor, pyroelectric detector, scandium aluminum nitride, aluminum nitride, CMOS compatible, non-dispersive infrared

1. INTRODUCTION

Sulfur hexafluoride (SF_6) gas is commonly used as insulating gas in high voltage transmission systems[1-2] due to its superior insulating properties.[3-4] Despite its advantageous properties in electrical insulating systems, SF_6 poses a threat to the environment by being a potent greenhouse gas, having the ability to trap infrared radiation 23,500 times more than carbon dioxide (CO_2).[5] Replacement of SF_6 with alternative non-greenhouse gases have been rigorously researched on[6-7] with SF_6 mixed in nitrogen (N_2)[8-10] as an alternative effort to dilute the concentration of SF_6 used in electrical insulating systems. Concurrent to the effort of finding replacement gases or diluting SF_6, it is important to identify and prevent SF_6 leakage into the environment.

We develop an optical-based SF_6 gas sensor based on complementary metal-oxide-semiconducter (CMOS) compatible pyroelectric detectors[11-16] to measure SF_6 gas at different concentrations mixed with N_2. The pyroelectric sensing layer used in this work for SF_6 gas sensing is aluminum nitride (AlN) and 12% scandium aluminum nitride (ScAlN) respectively. Application includes monitoring inline SF_6 or SF_6-in-N_2 gases to pick up signs of SF_6 leakage into the environment. Using non-dispersive infrared (NDIR) principle,[17-20] a wide range of SF_6 gas concentrations can be detected based on mid-infrared (IR) absorption of SF_6 at 10.6 µm wavelength. Moreover, no gas sensitive layer required in this sensor allows it to be immune to poisoning, hence enabling longer sensor lifetime and wider concentration range for detection from ppm to percentage levels.

SF_6 gas sensing response is measured using AlN-based pyroelectric detector and 12% ScAlN-based pyroelectric detector respectively. The output signals measured show that the gas sensor using 12% ScAlN-based pyroelectric detector gives a higher output signal (~73% higher at 100% SF_6 gas concentration) compared to AlN-based pyroelectric detector. Using

*Doris_NG@ime.a-star.edu.sg; phone 65 6826 6111; www.a-star.edu.sg/ime

N_2 as the reference gas, 12% ScAlN-based pyroelectric detector also shows a greater voltage drop (up to 2x) when sensing SF_6 gas. The time taken to response to SF_6 gas concentration is also measured and the results show that when using AlN-based pyroelectric detector, the gas response time (t_{90}) is ~6.26 s whereas a faster t_{90} ~ 1.99 s is observed when using 12% ScAlN-based pyroelectric detector. Both pyroelectric detectors' outputs are also measured across frequencies up to 40 Hz to identify their 3 dB roll-off frequency range to better understand the optimal frequencies that the detectors would function at. The SF_6 gas sensor in this work could potentially function as an inline sensor (for high concentration sensing) and a leakage sensor (for low concentration sensing). This sensor based on NDIR principle has advantages of being highly selective to SF_6 sensing in addition to being immune to poisoning, allowing longer lifetime and accurate monitoring of SF_6 gas concentration real time in an effort to mitigate SF_6 greenhouse gas leakage into the environment.

2. EXPERIMENTAL

The pyroelectric detectors used for SF_6 gas sensing in this paper are based on CMOS compatible pyroelectric sensing materials – AlN and 12% Sc-doped AlN. Both pyroelectric detectors have top and bottom electrodes (titanium nitride (TiN) and molybdenum (Mo) respectively) above and beneath the pyroelectric sensing layer, a bottom thermal insulating silicon dioxide (SiO_2) layer and a topmost absorber stack consisting of SiO_2 and silicon nitride (SiN) to absorb incoming light from the emitter source. Details on fabrication of AlN-based and 12% ScAlN-based pyroelectric detectors have been reported previously.[21-23]

Figure 1 shows a schematic of the exploded view of the SF_6 gas sensor. The sensor consists of 3 main components – a broadband emitter source emitting from wavelength range 2-14 µm, a 10 cm through-hole gas channel with diameter 5 mm and a CMOS compatible pyroelectric detector with AlN or 12% ScAlN as the pyroelectric sensing layer. These 3 main components used in the gas sensor set up is similar to that in Ref.[18] Optical bandpass filters used in this work is selected to be at SF_6 molecular fingerprint region (wavelength ~ 10.6 µm). They are arranged on the 2 ends of the gas channel, separating the gas channel from the source and detector. This is to allow light of wavelength ~10.6 µm to pass through the gas channel and interact with the SF_6 gas that will flow in the gas channel. The pyroelectric detector is placed on one end of the 10 cm gas channel while the other end of the gas channel consists of a thermal emitter source modulating at ~17.4 Hz powered using printed circuit board (PCB) connected by a universal serial bus (USB) cable. When SF_6 gas passes through the gas channel, it will absorb the 10.6 µm light that is in the gas channel, resulting in the detector sensing a lower voltage. SF_6 gas concentration can then be determined based on the drop in signal from the detector. To extract signal from the pyroelectric detector, it is connected to a current amplifier with gain 10^9 V/A and then a lock-in amplifier.

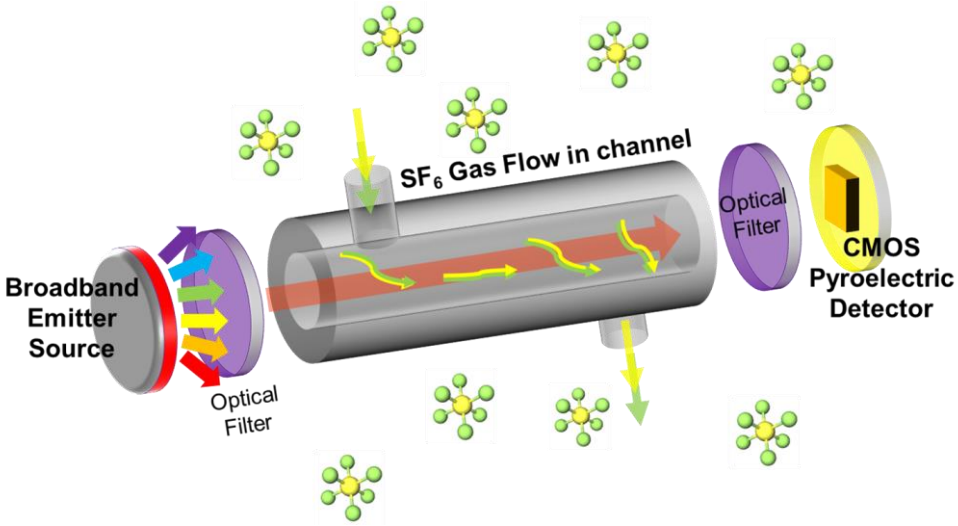

Figure 1. Schematic showing exploded view of our SF_6 gas sensor based on NDIR technique with broadband emitter source, gas channel where the SF_6 gas of different concentrations flow through and CMOS pyroelectric detector based on AlN or 12% ScAlN as the pyroelectric sensing layer.

3. RESULTS AND DISCUSSION

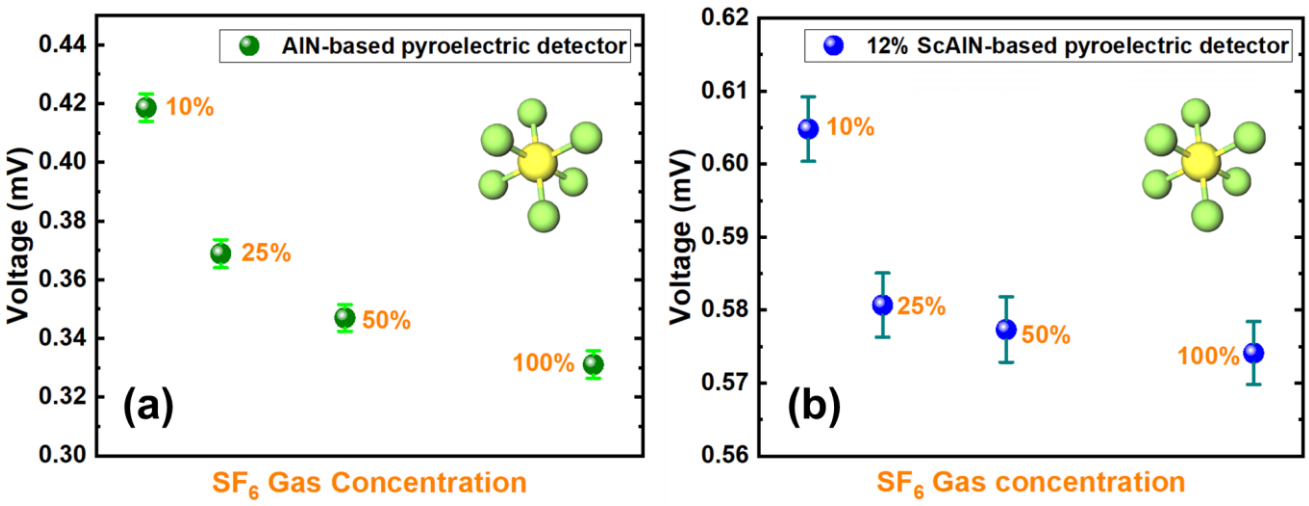

Figure 2. Output voltages measured from different gas concentrations of SF_6 mixed in N_2 when measured with (a) AlN-based and (b) 12% ScAlN-based pyroelectric detector respectively.

Figure 2 shows the output voltages measured when different concentrations of SF_6 passes through the gas channel using AlN-based pyroelectric detector (Fig. 2a) and 12% ScAlN-based pyroelectric detector (Fig. 2b) respectively. We tested at 4 different concentrations of SF_6 gas - 10%, 25%, 50% and 100%. The results show that as SF_6 gas concentration increases, the output signal received by both pyroelectric detectors reduces. This agrees well with NDIR principle where the molecular fingerprint of SF_6 lies at ~10.6 µm wavelength and that the gas absorbance of light occurs around this wavelength. With increase in SF_6 gas concentration, the presence of more molecules of SF_6 will increase absorption, resulting in less light (at ~10.6 µm) reaching the detector, hence lowering the voltage output signal. The gas sensing trend is however not linear as saturation will occur when the SF_6 gas molecules keep increasing. This can be noted with the reduced voltage drop from 50%-100% SF_6 gas concentration as compared to from 10%-50% in Fig. 2.

At 10% SF_6 gas concentration, the voltage measured from AlN-based pyroelectric detector is lower (~0.42 mV) than the voltage measured from 12% ScAlN-based pyroelectric detector (~0.605 mV). At 100% SF_6 gas concentration, the gas sensor using 12% ScAlN-based pyroelectric detector exhibits ~73% higher output signal compared to when AlN-based pyroelectric detector is used.

We further explore the voltage difference between N_2 (reference gas) and different SF_6 concentrations for respective pyroelectric detectors. Figure 3 shows the voltage differences between N_2 and respective concentrations of SF_6 gas for AlN-based and 12% ScAlN-based pyroelectric detectors. The voltage drop from N_2 when sensing SF_6 gas is greater (up to 2x) for 12% ScAlN-based pyroelectric detector compared to AlN-based pyroelectric detector. At 10% SF_6 gas concentration, AlN-based pyroelectric detector reads ~0.346 mV voltage drop (Fig. 3a) while 12% ScAlN-based pyroelectric detector reads ~0.719 mV voltage drop (Fig. 3b). We however note that from 10% SF_6 to 100% SF_6 gas concentration, the voltage drop difference for 12% ScAlN-based pyroelectric detector is lower (~0.0307 mV) compared to that of AlN-based pyroelectric detector (~0.0875 mV). This is further indication that saturation has kicked in for 12% ScAlN-based pyroelectric detector in sensing SF_6 after 25% gas concentration as the voltage drop after this gas concentration increases only slightly as observed by the gentler slope from Fig. 3b.

With 12% ScAlN-based pyroelectric detector exhibiting higher voltage drop at the same gas concentration compared to AlN-based pyroelectric detector, the limit of detection (LOD) for SF_6 gas using 12% ScAlN-based pyroelectric detector could be lower. Taking reference from Beer Lambert's equation,[24] we use Eq 1 to curve-fit the experimental data,

$$\Delta V(C) = \Delta V_{max}(1 - exp(-\gamma C))^m \quad (1)$$

where ΔV_{max} is the saturation voltage drop for a very large concentration, and $\gamma = \varepsilon L$ is the molar attenuation expressed in terms of molar attenuation coefficient ε and optical pathlength L. m denotes the pyroelectric activity which converts

incident optical power into voltage drop, which depends on the geometric and material parameters of the pyroelectric detector. Figure 3 shows the fitted data for AlN-based pyroelectric detector and 12% ScAlN-based pyroelectric detector using Eq. 1. When fitted, γ = 0.0357, ΔV_{max} = 0.435 mV, and m = 0.188 for AlN-based pyroelectric detector while γ = 0.0986, ΔV_{max} = 0.748 mV, and m = 0.0859 for 12% ScAlN-based pyroelectric detector. The experimental data is in good agreement with the fitting formula with coefficient of determination (R^2) very close to 1 for both detectors. The $m < 1$ in the fitting is consistent with the fact that there are still some inadequacies in Beer-Lambert's law (i.e. m = 1) wherein the relation between gas sensing output signal and gas concentration cannot be fully explained.[25-26] The noise in the pyroelectric measurement (σ) can then be used to estimate the limit of detection as LOD = $\gamma^{-1}(3\sigma/\Delta V_{max})^{1/m}$, where the 3σ estimate is used as a conservative estimate for LOD. More experimental data towards the lower concentrations will be required to further validate this curve-fitting.

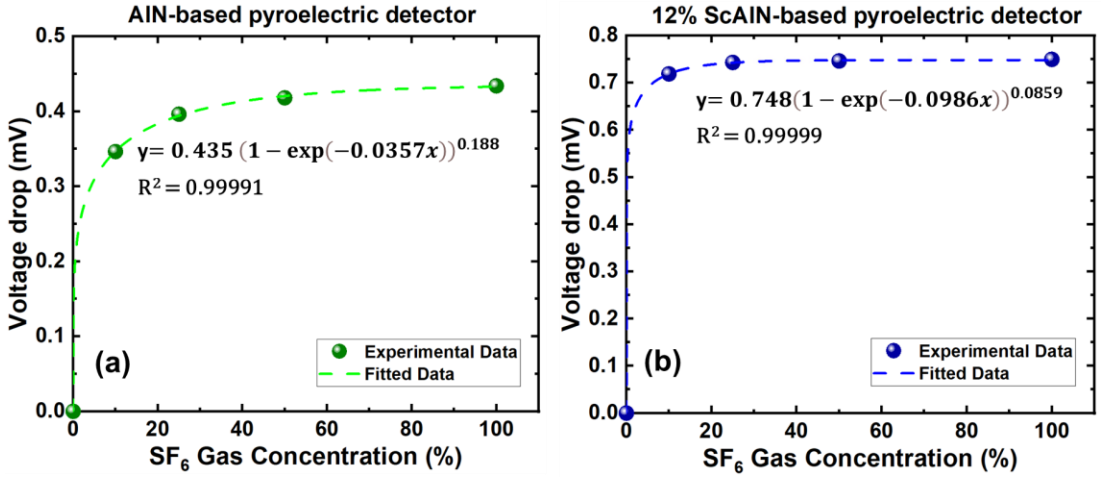

Figure 3. Plots showing voltage differences between N_2 and different concentrations of SF_6 for (a) AlN-based and (b) 12% ScAlN-based pyroelectric detectors.

Response times are measured to determine the time taken for the pyroelectric detectors to detect presence of SF_6 from a gas channel with N_2 gas running through it initially. Figure 4 shows t_{90} when the detector used is AlN-based pyroelectric detector (Fig. 5a) and 12% ScAlN-based pyroelectric detector (Fig. 4b) respectively. To detect 10% SF_6 gas from N_2 gas, t_{90} ~ 6.26 s for AlN-based pyroelectric detector and t_{90} ~ 1.99 s for 12% ScAlN-based pyroelectric detector. The response time for 12% ScAlN-based pyroelectric detector at ~2 s agrees with what was previously reported.[18-19] Response time for AlN-based pyroelectric detector is however longer with t_{90} ~ 6.26 s. This could be due to the higher percentage level SF_6 gas concentration used in the measurement in this work.

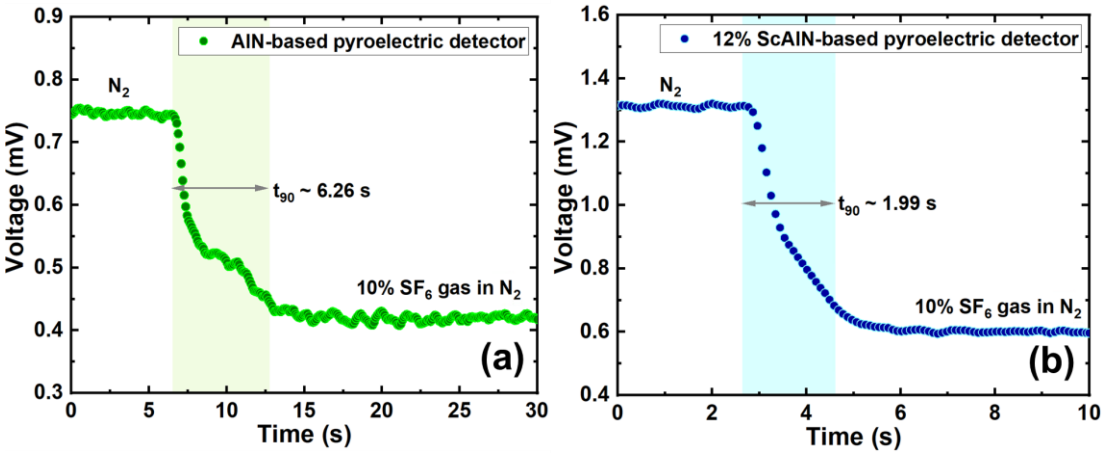

Figure 4. Time taken (t_{90}) for gas sensor with a) AlN-based and (b) 12% ScAlN-based pyroelectric detectors to response to 10% SF_6 gas concentration.

The electrical properties of both pyroelectric detectors are then measured at low frequencies up to 40 Hz to further understand their characteristics. Figure 5 shows the output amplitudes across different frequencies for (a) AlN-based and (b) 12% ScAlN-based pyroelectric detectors. The output amplitudes are plotted in dBV and their 3 dB roll-offs are measured. We note that 12% ScAlN-based pyroelectric detector yields higher peak amplitude (~ -53.03 dBV) compared to AlN-based pyroelectric detector (~ -54.02 dBV). This is most likely due to the higher pyroelectric coefficient from 12% Sc-doped AlN.[22,27] In terms of operational frequency, Fig. 5a shows that for AlN-based pyroelectric detector, the 3 dB roll-off cuts at ~13.5 Hz frequency while for 12% ScAlN-based pyroelectric detector, the 3 dB roll-off cuts at ~12.6 Hz, as seen from Fig. 5b. Optimal frequency range for AlN-based pyroelectric detector is ~5.6 Hz – 13.5 Hz (Fig. 5a) while that for 12% ScAlN-based pyroelectric detector is from ~5.2 Hz – 12.6 Hz (Fig. 5b) respectively. In this work, we operate our pyroelectric detectors at higher frequency ~17.4 Hz which is out of the 3 dB roll-off range. Despite that, we are able to get SF_6 gas sensing response. SF_6 gas sensing performance will further improve if the pyroelectric detectors operates within the 3 dB roll-off ranges shown in Fig. 5.

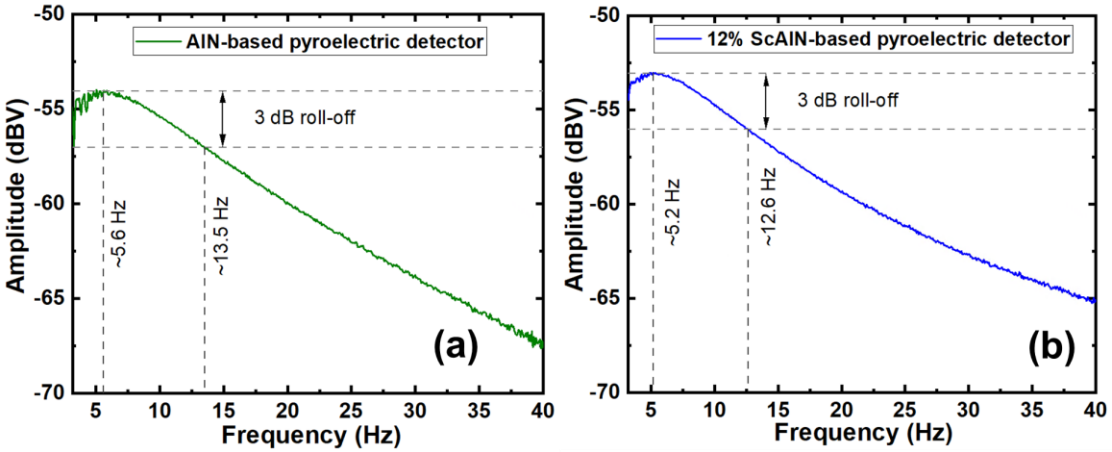

Figure 5. Output amplitude based on dBV of (a) AlN-based and (b) 12% ScAlN-based pyroelectric detectors plotted against frequency showing the 3 dB roll-off characteristics of both pyroelectric detectors.

4. CONCLUSION

In summary, we build a SF_6 gas sensor based on NDIR principle. CMOS compatible AlN-based and 12% ScAlN-based pyroelectric detectors are used in this gas sensor to measure the gas sensing response. A comparison is done on the performance of both detectors. We note that the gas sensor with 12% ScAlN-based pyroelectric detector presents a higher initial output voltage ~1.32 mV (in the presence of N_2) compared to AlN-based pyroelectric detector (~0.765 mV), exhibiting an increase ~73%. This increase of ~73% from 12% ScAlN-based pyroelectric detector is also observed at 100% SF_6 gas concentration. The voltage drop between N_2 and different concentrations of SF_6 is then measured and revealed up to 2x increase in voltage drop for 12% ScAlN-based pyroelectric detector compared to AlN-based pyroelectric detector when sensing 10% SF_6 gas concentration. Response time measured also shows that 12% ScAlN-based pyroelectric detector responds faster (t_{90} ~ 1.99 s) to 10% SF_6 gas concentration compared to AlN-based pyroelectric detector (t_{90} ~ 6.26 s). The electrical performance of both pyroelectric detectors are also examined across frequency up to 40 Hz to identify the 3 dB roll-off frequency range. We note that the 3 dB roll-off frequency range is from ~5.6-13.5 Hz for AlN-based pyroelectric detector and ~5.2-12.6 Hz for 12% ScAlN-based pyroelectric detector. The detectors used are CMOS compatible and could potentially allow for ease of integration with CMOS circuitries later on in the development. This SF_6 gas sensor based on NDIR principle is highly selective to sensing SF_6 gas as it senses based on SF_6 absorption at its molecular fingerprint wavelength ~10.6 µm which does not overlap with that of other gases. The sensor is also immune to poisoning as it does not require a gas sensitive layer which could affect the sensor useful lifetime. This SF_6 gas sensor system in this work will enable monitoring of SF_6 gas concentration real time in an effort to mitigate SF_6 greenhouse gas emission into the environment.

ACKNOWLEDGEMENTS

This research is supported by the National Research Foundation, Singapore, and A*STAR (Agency for Science, Technology and Research), Singapore under its Low-Carbon Energy Research (LCER) Funding Initiative (FI) (Award no.: U2102d2012) for testing and analysis and A*STAR (Agency for Science, Technology and Research), Singapore under RIE2020 Advanced Manufacturing and Engineering (AME) IAF-PP Grant with grant numbers A1789a0024 for fabrication.

REFERENCES

[1] Cai, W., Tang, J., Cheng, L., Zhang, C., Fan, M., Zhou, Q., Yao, Q., "Detection of SF_6 decomposition components under partial discharge by photoacoustic spectrometry and its temperature characteristic," IEEE Trans. Instrum. Meas. 65(6), 1343–1351 (2016).

[2] Milanovic, Z., Stankovic, K., Vujisic, M., Radosavljevic, R., Osmokrovic, P. "Calculation of impulse characteristics for gas-insulated systems with homogenous electric field," IEEE Trans. Dielectr. Elect. Insul. 19(2), 648–659 (2012).

[3] Lee, E. K., Lee, J. D., Lee, H. J., Lee, B. R., Lee, Y. S., Kim, S. M., Park, H. O., Kim, Y. S., Park, Y.-D., Kim, Y. D., "Pure SF_6 and SF_6-N_2 mixture gas hydrates equilibrium and kinetic characteristics," Environmental Science and Technology, 43(20), 7723-7727 (2009).

[4] Ibrahim, S. I., Jawad, E. A., Jassim, M. K., "Study the effect of mixing N_2 with SF_6 gas on electron transport coefficients," AIP Conference Proceedings, 2386, 070003 (2022).

[5] National Grid Group. *What is SF6? Sulphur hexafluoride explained*. [online] Available at: https://www.nationalgrid.com/stories/energy-explained/what-is-sf6-sulphur-hexafluoride-explained#:~:text=SF6%20is%20one%20of,over%20longer%20periods%20of%20time. [Accessed 6 January 2024].

[6] Xiao, S., Zhang, X., Tang, J., Liu, S., "A review on SF_6 substitute gases and research status of CF_3I gases," Energy Reports, 4, 486-496 (2018).

[7] Tian, S., Zhang, X., Cressault, Y., Hu, J., Wang, B., Xiao, S., Li, Y., Kabbaj, N., "Research status of replacement gases for SF_6 in power industry," AIP Advances, 10, 050702 (2020).

[8] Qu, B., Yang, Q., Li, Y., Malekian, R., Li, Z., "A new concentration detection system for SF_6/N_2 mixture gas in extra/ultra high voltage power transmission systems," IEEE Sensors Journal, 18(9) 3806-3812 (2018).

[9] Wang, Y., Liang, J. Q., Yu, C. L., Li, L., Zhang, H. D., Li, G. X., "Research on the synergy of SF_6/N_2 mixture gas in low temperature environment," IOP Conf. Series: Materials Science and Engineering, 479, 012045 (2019).

[10] Hou, Z., Guo, R., He, C., Li, J., Yao, X., "Synergistic effect of SF_6/N_2 gas mixtures on surface partial discharge under DC voltage," IEEE Transactions on Dielectrics and Electrical Insulation, 27(2), 692-699 (2020).

[11] Ranacher, C., Consani, C., Tostschanoff, A., Rauter, L., Holzmann, D., Fleury, C., Stocker, G., Fant, A., Schaunig, H., Irsigler, P., Grille, T., Jakoby, B., "A CMOS compatible pyroelectric mid-infrared detector based on aluminium nitride," Sensors, 19, 2513 (2019).

[12] Lehmkau, R., Mutschall, D., Kaiser, A., Ebermann, M., Neumann, N., Czernohorsky, M., Neuber, M., Hiller, K., Seiler, J., Großmann, T. D., "Fully CMOS-compatible pyroelectric infrared detector based on doped HfO_2 thin film in 3D-integration," Proc. SPIE 12002, Oxide-based Materials and Devices XIII, 120020M (2022).

[13] Ranu, B, U., Sinha, R., Agarwal, P. B., "CMOS compatible pyroelectric materials for infrared detectors," Materials Science in Semiconductor Processing, 140, 106375 (2022).

[14] Ng, D. K. T., Ho, C. P., Xu, L., Chen, W., Fu, Y. H., Zhang, T., Siow, L. Y., Jaafar, N., Ng, E. J., Gao, Y., Cai, H., Zhang, Q., Lee, L. Y. T., "CO_2 gas sensing by CMOS-MEMS ScAlN-based pyroelectric detector based on mid-IR absorption," 2021 21st International Conference on Solid-State Sensors, Actuators and Microsystems (Transducers), Orlando, FL, USA, 827-830 (2021).

[15] Ng, D. K. T., Ho, C. P., Zhang, T., Xu, L., Siow, L. Y., Chung, W. W., Cai, H., Lee, L. Y. T., Zhang, Q., Singh, N., "CMOS compatible MEMS pyroelectric infrared detectors: from AlN to ScAlN," Proc. SPIE 11697, MOEMS and Miniaturized Systems XX, 116970N (2021).

[16] Xu, L., Ng, D. K. T., Chen, W., Li, N., Ho, C. P., Goh, D. J., Zhang, Y., Zhang, Q., Lee, L. Y. T., "Low-power contactless button system based on MEMS ScAlN pyroelectric detector," Proc. SPIE 12434, MOEMS and Miniaturized Systems XXII, 1243405 (2023).
[17] Tan, X., Zhang, H., Li, J., Wan, H., Guo, Q., Zhu, H., Liu, H., Yi, F., "Non-dispersive infrared multi-gas sensing via nanoantenna integrated narrowband detectors," Nature Communications, 11, 5245 (2020).
[18] Ng, D. K. T., Xu, L., Fu, Y. H., Chen, W., Ho, C. P., Goh, J. S., Chung, W. W., Jaafar, N., Zhang, Q., Lee, L. Y. T., "CMOS AlN and ScAlN pyroelectric detectors with optical enhancement for detection of CO_2 and CH_4 gases," Adv. Electron. Mat. 9, 2300256 (2023).
[19] Ng, D. K. T., Ho, C. P., Xu, L., Chen, W., Fu, Y. H., Zhang, T., Siow, L. Y., Jaafar, N., Ng, E. J., Gao, Y., Cai, H., Zhang, Q., Lee, L. Y. T., "NDIR CO_2 gas sensing using CMOS compatible MEMS ScAlN-based pyroelectric detector," Sensors and Actuators: B. Chemical, 346, 130437 (2021).
[20] Ng, D. K. T., Xu, L., Chen, W., Wang, H., Gu, Z., Chia X. X., Fu, Y. H., Jaafar, N., Ho, C. P., Zhang, T., Zhang, Q., Lee, L. Y. T., "Miniaturized CO_2 Gas Sensor using 20% ScAlN-based pyroelectric detector," ACS Sensors, 7, 2345-2357 (2022).
[21] Ng, D. K. T., Wu, G., Zhang, T. –T., Xu, L., Sun, J., Chung, W. –W., Cai, H., Zhang, Q., Singh, N., "Considerations for an 8-inch wafer-level CMOS compatible AlN pyroelectric 5-14 μm wavelength IR detector towards miniature integrated photonics gas sensors," Journal of Microelectromechanical Systems, 29 (5), 1199-1207 (2020).
[22] Ng, D. K. T., Zhang, T., Siow, L. Y., Xu, L., Ho, C. P., Cai, H., Lee, L. Y. T., Zhang, Q., Singh, N., "A functional CMOS compatible MEMS pyroelectric detector using 12%-doped scandium aluminum nitride," Applied Physics Letters, 117, 183506 (2020).
[23] Ng, D. K. T., Ho, C. P., Xu, L., Zhang, T., Siow, L. Y., Ng, E. J., Cai, H., Zhang, Q., Lee, L. Y. T., "CMOS-MEMS $Sc_{0.12}Al_{0.88}N$-based pyroelectric infrared detector with CO_2 gas sensing," 2021 IEEE 34th International Conference on Micro Electro Mechanical Systems (MEMS), Gainesville, FL, USA, 852-855, (2021).
[24] Pfeiffer, H. G., Liebhafsky, H. A., "The origins of Beer's law," Journal of Chemical Education, 28(3), 123 (1951).
[25] Mayerhöer, T. G., Pahlow, S., Popp, J., "The Bouguer-Beer-Lambert law: Shining light on the obsure," ChemPhysChem, 21, 2029-2046 (2020).
[26] Mayerhofer, T. G., "Understanding the limits of the Bouguer-Beer-Lambert law," Spectroscopy, 38(8), 29-30, 58 (August 2023).
[27] Ng, D. K. T., Zhang, T., Siow, L. Y., Xu, L., Ho, C. P., Cai, H., Lee, L. Y. T., Zhang, Q., Singh, N., "Improved specific detectivity to 10^7 for CMOS-MEMS pyroelectric detector based on 12%-doped scandium aluminum nitride," 2021 IEEE 34th International Conference on Micro Electro Mechanical Systems (MEMS), Gainesville, FL, USA, 860-863, (2021).